Pacific Northwest
NATIONAL LABORATORY

PNNL-38317

Remote Sensing Approach for Monitoring Tree Health Adjacent to Transmission Corridors

September 2025

Kyle B. Larson
Victoria M. Sinnott
André M. Coleman

U.S. DEPARTMENT of ENERGY

Prepared for the U.S. Department of Energy
under Contract DE-AC05-76RL01830

DISCLAIMER

PACIFIC NORTHWEST NATIONAL LABORATORY
operated by
BATTELLE
for the
UNITED STATES DEPARTMENT OF ENERGY
under Contract DE-AC05-76RL01830

Printed in the United States of America

Available to DOE and DOE contractors from
the Office of Scientific and Technical Information,
P.O. Box 62, Oak Ridge, TN 37831-0062
www.osti.gov
ph: (865) 576-8401
fox: (865) 576-5728
email: reports@osti.gov

Available to the public from the National Technical Information Service
5301 Shawnee Rd., Alexandria, VA 22312
ph: (800) 553-NTIS (6847)
or (703) 605-6000
email: info@ntis.gov
Online ordering: http://www.ntis.gov

PNNL-38317

Remote Sensing Approach for Monitoring Tree Health Adjacent to Transmission Corridors

September 2025

Kyle B. Larson
Victoria M. Sinnott
André M. Coleman

Prepared for
the U.S. Department of Energy
under Contract DE-AC05-76RL01830

Pacific Northwest National Laboratory
Richland, Washington 99354

Abstract

This study presents an initial proof-of-concept for a satellite-based remote sensing approach to identify and monitor potential areas of poor tree health across the entire BPA service territory on an annual basis. We tested three variants of "delta peak NDVI" (ΔPN) change detection metrics that express interannual variation in primary productivity relative to a baseline by comparing ΔPN values for known insect/disease disturbances and nearby reference locations. All three metrics showed promise for detecting poor tree health in the year during disturbance, but the metric based on the difference from the long-term (2016-2024) median ($\Delta_{Med}PN$) was preferred due to its responsiveness to change in the years during and after disturbance, resilience to interannual variation, and ease of interpretation as being above or below normal. Comparison of $\Delta_{Med}PN$ grouped by relative severity of disturbance indicated it was not sensitive enough to detect "low" severity disturbances, as mapped by USGS's LANDFIRE program, but could distinguish "moderate" and "high" severity disturbances from reference locations. These findings informed the selection of a threshold for $\Delta_{Med}PN$, which was combined with areas exhibiting negative NDVI to map potential areas of concern. Visual inspection of high-resolution imagery before and after, as well as NDVI time series, revealed that many areas of concern corresponded to visible signs of defoliation and die-off, as well as other types of disturbances (e.g., landslides, logging, road grading, flooding). Some areas of concern are believed to be false detections caused by persistent shadows, and others could not be explained through visual inspection due to the spatiotemporal limitations of before-and-after imagery. In summary, our approach shows promise for large-scale monitoring of tree health adjacent to BPA transmission lines; however, additional work is recommended to enhance model sophistication and reduce noise.

Acknowledgments

The Pacific Northwest National Laboratory team would like to recognize and thank Jeff Cook, Kelly Miller, Matt Weaver, James Hillegas-Elting, Chuck Sheppard, John Tyler, Rebecca Woods, Amber Churchill, Jessica Simmons, and the rest of the Bonneville Power Administration wildfire team for their valuable leadership and insights to the development of this remote sensing approach for monitoring tree health adjacent to BPA transmission.

Acronyms and Abbreviations

BPA	Bonneville Power Administration
DW	Dynamic World
EO	Earth Observation
ESA	European Space Agency
GEE	Google Earth Engine
LiDAR	Light Detection and Ranging
NAIP	National Agriculture Imagery Program
NDVI	Normalized Difference Vegetation Index

Contents

Abstract ii
Acknowledgments iii
Acronyms and Abbreviations iv
1.0 Introduction 1
2.0 Methods 2
2.1 Spectral Measures of Vegetation Productivity 2
2.2 Evaluation of Change Metrics 5
2.3 Identification and Evaluation of Areas of Concern 7
3.0 Results & Discussion 9
3.1 Delta Peak NDVI Change Metrics 9
3.2 Delta Peak NDVI Threshold 10
3.3 Areas of Concern 11
4.0 Conclusions 7
5.0 References 8

Figures

Figure 1. Illustration of three delta peak NDVI metrics: delta 2016 ($\Delta 2016PN$), delta year before ($\Delta t-1PN$), and long-term (2016-2024) median annual peak NDVI ($\Delta MedPN$). 4
Figure 2. Locations of LANDFIRE-mapped “insects/disease” disturbances (red points) within 500-m of BPA transmission lines (blue lines). 5
Figure 3. Example map of LANDFIRE-mapped “insect/disease” disturbances within 500-m of BPA transmission lines across multiple years. 6
Figure 4. Example map of reference locations relative to known insect and disease disturbances between 2017-2022. The map on the left displays a segment of a BPA transmission corridor along with disturbances recorded from 2017 to 2022. Red triangles indicate randomly generated points representing reference locations. The map on the right provides a zoomed-in view showing how each undisturbed location was paired with its nearest disturbance for further analysis. 7
Figure 5. The central map shows where the POAN-SAPO and GARR-TAFT transmission lines relative to other BPA transmission Lines . The left map highlights POAN_SAPO line segments (miles 26-36), and the right map highlights GARR-TAFT line segments (miles 38-49), which were identified by BPA as areas with signs of unhealthy vegetation. 8
Figure 6. Boxplots of three different ΔPN change metrics for LANDFIRE-mapped insect/disease disturbances. Plots are organized from left to right by metric: delta long-term median ($\Delta MedPN$), delta year before ($\Delta t-1PN$),

and delta 2016 ($\Delta 2016PN$); and top to bottom by disturbance severity (low, medium, high). 10

Figure 7. Boxplots of zonal mean $\Delta MedPN$ in the year before, during, and after for LANDFIRE-mapped “insect/disease” disturbances (top row) and undisturbed reference locations (bottom row). Plots are further categorized from left to right by low, medium, and high severity. Blue dashed lines connect boxplot medians, the whiskers represent the 5th and 95th percentiles, and the dots represent outliers beyond those percentiles. 11

Figure 8. Example area of concern near POAN-SAPO line (124.118168° W, 48.109578° N). NDVI time series corresponds to location of green pin and indicates decline in tree health began between 2021 and 2022. Comparison of NAIP imagery from 2017 (top) and 2023 (bottom) shows expansion of tree defoliation and die-off. 12

Figure 9. Example area of concern near POAN-SAPO line (124.014879° W, 48.096417° N). NDVI time series corresponds to location of green pin and indicates decline in tree health began as early as 2019 but accelerated between 2023 and 2024. Comparison of NAIP imagery from 2017 (top) and 2023 (bottom) shows increasing severity of tree defoliation and die-off. 13

Figure 10. Example area of concern near GARR-TAFT line (113.661686° W, 46.696434° N). NDVI time series corresponds to location of green pin and indicates decline in tree health occurred between 2022 and 2023. Comparison of NAIP imagery from 2021 (top) and 2023 (bottom) shows expansion of tree defoliation and die-off. 1

Figure 11. Example area of concern near GARR-TAFT line (113.596140° W, 46.687284° N). NDVI time series corresponds to location of green pin and indicates decline in tree health occurred between 2021 and 2023. Comparison of NAIP imagery from 2021 (top) and 2023 (bottom) shows appearance of tree defoliation and die-off. 2

Figure 12. Example area of concern near POAN-SAPO line (124.143765° W, 48.099868° N). NDVI time series corresponds to location of green pin and indicates decline in tree health occurred between 2021 and 2022. Comparison of NAIP imagery from 2019 (top) and 2023 (bottom) shows appearance of a landslide. 3

Figure 13. Example area of concern near GARR-TAFT line (113.673946° W, 46.702911° N). NDVI time series corresponds to location of green pin and indicates decline in tree health occurred between 2021 and 2023. Comparison of NAIP imagery from 2021 (top) and 2023 (bottom) shows loss of vegetation and tree die-off due to flood scarring. 4

Figure 14. Example area along POAN-SAPO line where persistent shadow is believed to cause false-positive detection. 5

Figure 15. Example non-forested areas where Dynamic World land cover is misclassified as “tree”. Background image is 2023 NAIP. 6

1.0 Introduction

Every year, the Bonneville Power Administration (BPA) experiences outages due to trees falling on transmission infrastructure, commonly referred to as vegetation fall-in. While many vegetation fall-in incidents are linked to high wind events, post-event inspections often reveal that poor tree health may be a contributing factor to blowdown. Tree health may be impacted for a variety of reasons and over varying time scales. For example, tree health may decline gradually over time due to factors such as prolonged drought, aging/succession, pests, disease, or fungal root rot. Additionally, tree health may decline rapidly within a growing season due to factors like wildfire, wind shear, or human disturbance. Regardless, identifying where unhealthy trees are located versus why they are unhealthy represents first- and second-order challenges for BPA, forest managers, and researchers alike.

BPA maintains thousands of miles of transmission lines that span six Northwest states and a diverse range of forest ecosystems with varying degrees of remoteness; thus, the practical challenges alone to identifying the location of unhealthy trees represent a daunting task for BPA. To complicate matters further, the timeframe between when at-risk trees are identified and when preventative action can be taken by BPA can be a months-long process, resulting in missed opportunities and damaging tree-fall events. Remote sensing applications are ideal for this problem, as they enable wide-area surveillance at comparatively lower costs than ground-based methods. BPA does collect super-resolution (0.3 – 1 m) LiDAR (Light Detection and Ranging) and true-color imagery for its transmission lines, although due to cost and laborious nature of data collection and post-processing, it is only able to collect data for a given area approximately every 3 years, which may be too infrequent to detect certain changes. Conversely, satellite-based remote sensing offers much higher revisit rates (approximately weekly but up to daily) and wider geographic coverage, making it well-suited for identifying short-term change over large landscapes. Many sources of satellite imagery are open-access/ publicly available. However, the spatial resolution of public satellite imagery (10-30 m) is insufficient for identifying individual unhealthy trees.

This report describes a pilot effort to develop a satellite-based remote sensing approach for identifying and monitoring potential areas of poor tree health across the entire BPA service territory on an annual basis. The approach aims to identify thresholds of change in vegetation productivity for both within-year and following-year time scales, which can serve as early indicators of disturbance. These thresholds are developed with the aid of 25 years of disturbance data and 10 years of satellite imagery. Furthermore, the method of change detection is agnostic to the underlying cause of disturbance, making it more robust to detecting changes in tree health across the geographically expansive and ecologically diverse BPA service territory.

2.0 Methods

Here, we describe our remote sensing approach for identifying and monitoring potential areas of poor tree health adjacent to BPA transmission corridors. The overall approach can be summarized as follows:

- Convert satellite-based spectral measures of vegetation productivity over time to metrics that reflect change relative to short- and long-term baselines.
- Compare change metrics between known areas of disturbance and reference locations with little to no disturbance to determine a threshold for flagging areas of concern.
- Combine metric thresholding with vegetation productivity trend analysis to identify areas of concern and approximate the time when the disturbance occurred.
- Visually compare pre- and post-disturbance imagery for areas of concern to qualitatively assess the efficacy of our method.

Each of these steps is described in greater detail in the following sections. All satellite imagery was acquired and analyzed using Google Earth Engine (GEE), which is a multi-petabyte cloud-based planetary data analysis platform that enables rapid and scalable remote sensing workflows over long time series.

2.1 Spectral Measures of Vegetation Productivity

Our method for assessing vegetation health centers on the use of Earth Observation (EO) satellite imagery, specifically that provided by the European Space Agency's (ESA) Sentinel-2 mission which began in June 2015. This EO satellite is well-suited for measuring changes in vegetation health, productivity, biomass, and other characteristics across large areas because it has a sun-synchronous (daytime) orbit pattern, high revisit rate (every 5 days), large image footprints (~10,000 km^2), high spatial resolution (10 x 10 meters), and contain sensors that detect light in both the visible and non-visible portions of the electromagnetic spectrum. The latter capability is especially useful for exploiting the unique spectral characteristics of vegetation. One common method that leverages both visible and non-visible information is the Normalized Vegetation Difference Index (NDVI), which serves as a proxy measure of vegetation health.

NDVI is a unitless index that relates to photosynthetic activity, with values ranging from -1 to 1, where 1 represents maximum photosynthetic activity (informally referred to as "greenness") and -1 represents minimum photosynthetic activity. NDVI values also differ significantly across different types of vegetation (e.g., grassland vs. forest, evergreen vs. broadleaf) and throughout the growing season as vegetation greens up and senesces. To mitigate these factors, we first derived annual peak NDVI measures by compositing all Sentinel-2 images for a given year into a single image where each pixel value represents the maximum NDVI measured at that location throughout the year. This method of compositing imagery achieves three key improvements compared to single-date imagery. First, it creates an image representing vegetation at peak productivity, making comparisons of inter-annual images more interpretable and less influenced by within-season variability. Second, it effectively creates a cloud-free and snow-free image, thereby improving overall coverage. Finally, it provides a basis for establishing baseline measures that are less susceptible to interannual variability in temperature and precipitation.

This latter characteristic is key to the second way in which we mitigate variability in NDVI, which is to difference the annual peak NDVI from short- and long-term baselines, resulting in annual change metrics that represent whether productivity is above or below the baseline. We refer to these metrics as “delta peak NDVI” (ΔPN). Three baseline periods were selected for testing different delta peak NDVI metrics, each with different sets of advantages and disadvantages: delta 2016 ($\Delta_{2016}PN$), delta year before ($\Delta_{t-1}PN$), and long-term (2016-2024) median annual peak NDVI ($\Delta_{Med}PN$) (Figure 1). We chose the median instead of mean annual peak NDVI because the former is less sensitive to outliers and therefore a better indicator of long-term central tendency. The key advantage of the 2016 delta peak NDVI metric ($\Delta_{2016}PN$) is that it provides a static baseline from the time Sentinel-2 collection began. However, due to its arbitrary nature, its utility as a baseline may vary spatially depending on whether local conditions were wetter or drier, or cooler or hotter than normal in 2016. Conversely, the year before the delta peak NDVI metric ($\Delta_{t-1}PN$) is a dynamic metric that may be more sensitive to short-term change, but like $\Delta_{2016}PN$, it does not account for interannual variation in productivity due to climatic conditions. The long-term median delta NDVI metric $\Delta_{Med}PN$ is a static metric that accounts for interannual variation in productivity due to climatic conditions and can be interpreted more straightforwardly than the other metrics; however, it may be less sensitive to detecting subtle change that is within the range of normal variation.

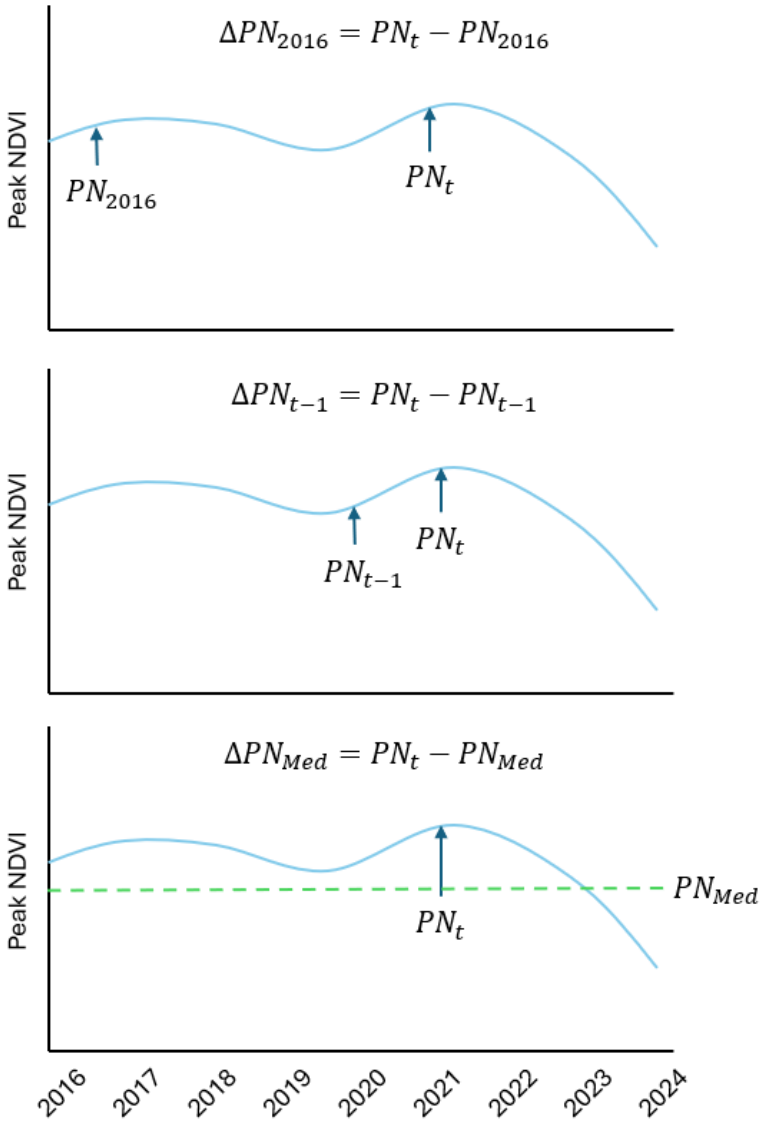

Figure 1. Illustration of three delta peak NDVI metrics: delta 2016 ($\Delta_{2016}PN$), delta year before ($\Delta_{t-1}PN$), and long-term (2016-2024) median annual peak NDVI ($\Delta_{Med}PN$).

Image analysis was constrained in three ways: temporally, spatially, and ecologically. When compositing imagery, we used Sentinel-2 images spanning the growing season (March 1 to November 30) and time of peak productivity for most forest associations in the study area. Spatially, we constrained image analysis to a 500-m buffer around all BPA transmission lines, as we are interested in detecting tree health anomalies that may affect BPA infrastructure. Finally, we constrained image analysis to forest vegetation types using Dynamic World (DW) land cover data, a global 10-m resolution near-real-time land cover dataset derived from the entire Sentinel-2 satellite image catalog (Brown et al., 2022). We created annual and 8-year tree mask layers by compositing DW time series land cover data based on the most common land cover class for each pixel within each year and across years 2016-2024. Although Sentinel-2 collection began in June 2015, our dataset begins in 2016 because it is the first full year of Sentinel-2 collection that spans our target growing season (March 1 to November 30).

2.2 Evaluation of Change Metrics

To evaluate the sensitivity of ΔPN metrics for detecting poor tree health, we compare ΔPN trends for forest areas with and without contemporary disturbances as mapped by the U.S. Geological Survey's (USGS's) LANDFIRE program, LF 2023 release. LANDFIRE maps multiple types of disturbance (e.g., wildfire, insects/disease, mechanical, windthrow, and mastication) and estimates the year a disturbance occurred and its relative severity (i.e., low, moderate, high). It is worth noting there is some uncertainty in the accuracy of LANDFIRE disturbance type, year, and severity, including how severity levels correspond to observable defoliation or die-off. LANDFIRE disturbance boundaries are also generalized during the mapping process. Given these considerations, we expect there to be significant variation in ΔPN for LANDFIRE-mapped disturbances.

Theoretically, ΔPN should be sensitive to any disturbance that affects tree health; however, we focus on disturbances classified as "insects/disease" because we are interested in elucidating thresholds of change for areas that experience gradual defoliation and die-off, as these are more difficult to detect. We selected LANDFIRE-mapped "insects/disease" disturbances that occurred between 2017 and 2023 within 500 m of BPA transmission lines that were greater than 900 m^2 (N=1877; Figure 2 and Figure 3), which corresponds to approximately a 3x3 pixel area for Sentinel-2 imagery. This helps ensure that pixel values are less affected by variability in orbit position and georeferencing. Our disturbance dataset begins in 2017 because the $\Delta_{2016}PN$ and $\Delta_{t-1}PN$ change metrics are not applicable in 2016, the first year in our dataset, and ends in 2023 because that was the most recent year of disturbance data included in the LF 2023 release.

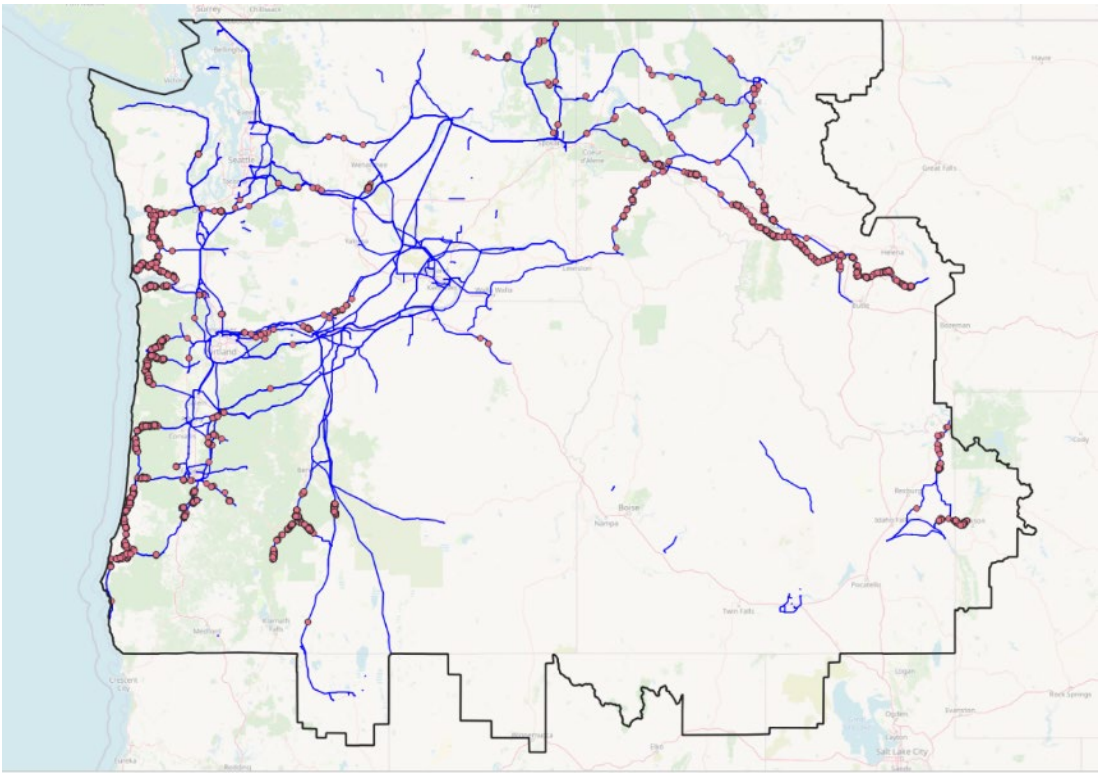

Figure 2. Locations of LANDFIRE-mapped "insects/disease" disturbances (red points) within 500-m of BPA transmission lines (blue lines).

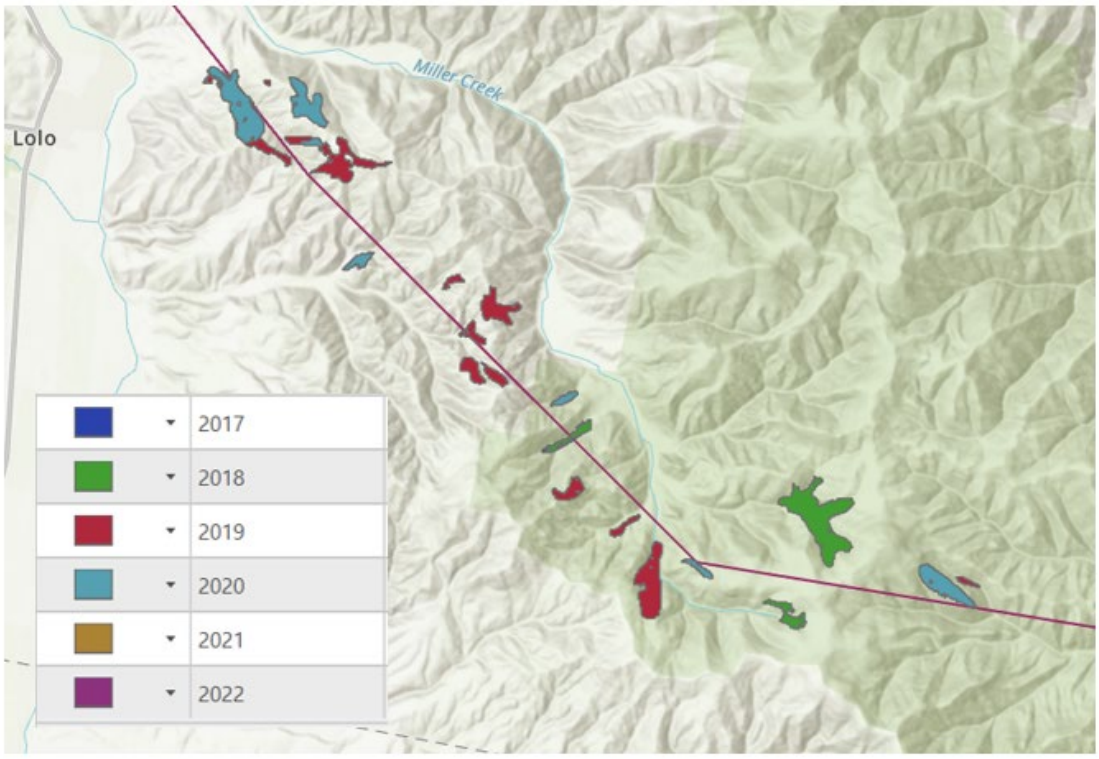

Figure 3. Example map of LANDFIRE-mapped “insect/disease” disturbances within 500-m of BPA transmission lines across multiple years.

Reference locations were identified by compositing all disturbances in LANDFIRE annual disturbance data from 1999 to 2023 and taking the inverse of those areas. These areas are assumed to have had little to no measurable disturbance in the past 24 years and thus are considered good reference locations for comparing change metrics in disturbed areas. Reference locations were selected by generating 100,000 random points in areas without known disturbance and then sub-setting them by the following criteria: within 1-5 km of insect/disease disturbances, 1 km of transmission corridors, and persistent tree cover, as per our DW decadal tree mask. This left 11,095 reference locations for use in our analysis.

To quantify and compare ΔPN metrics for known disturbances and reference locations, we used zonal statistics to calculate the mean and standard deviation ΔPN for all pixel values in each disturbed/reference location. Because reference locations are based on random points, we used a 38 m radius buffer, equivalent to the average area of disturbed locations (4,536 m² or 1.12 acres), for the zonal statistic calculation. Zonal mean ΔPN values for reference locations were paired with that of disturbances based on proximity and disturbance year (Figure 4); i.e., if the closest disturbance to a given reference location happened in 2018 and was classified as “low” severity, we used the zonal mean ΔPN value for 2018 for that reference location and assigned it to the “low” severity pool. We then generated boxplots of disturbed vs. reference ΔPN values stratified by disturbance severity to determine a threshold for ΔPN needed to detect a negative change in tree health. We suggest future work apply more rigorous statistical tests and modeling techniques, as well as incorporate other explanatory factors such as plant community, stand age, aspect, slope, elevation, etc., to refine the use of ΔPN thresholding.

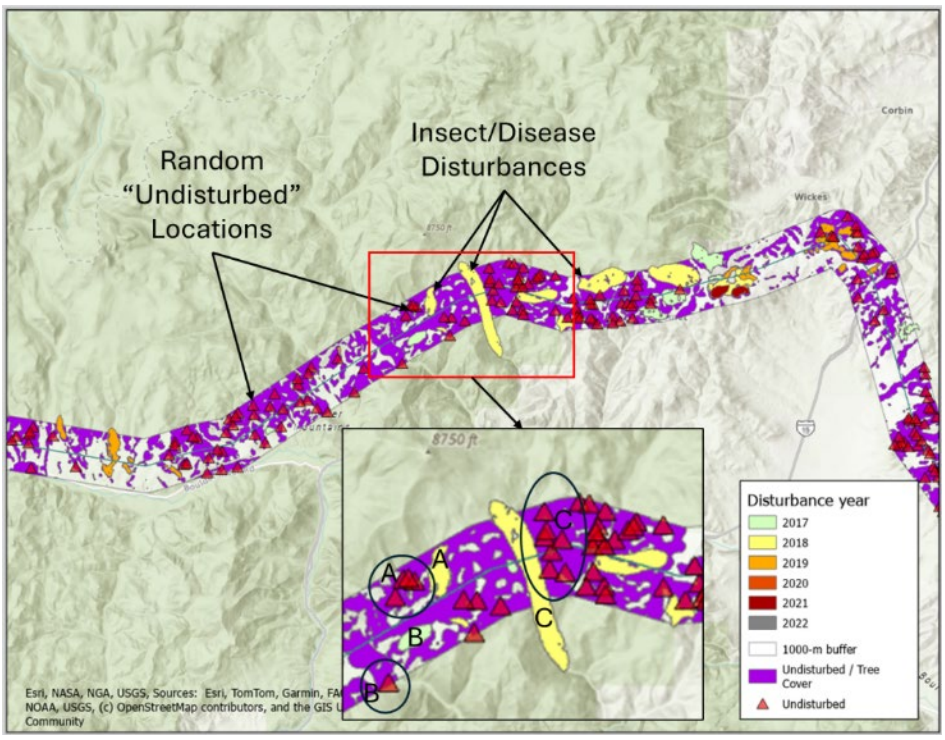

Figure 4. Example map of reference locations relative to insect/disease disturbances mapped by LANDFIRE between 2017-2023. Red triangles are randomly generated points representing reference locations. The inset map shows how each undisturbed location was paired with its nearest disturbance, as denoted by the labels A, B, and C.

2.3 Identification and Evaluation of Areas of Concern

We define an "area of concern" as any pixel with a negative NDVI trend between 2016-2024 and a ΔPN below the threshold of change (-0.045). The purpose of trend analysis is to better distinguish areas of temporary versus persistent decline in NDVI, while the ΔPN threshold is to identify areas that exhibit change that is indicative of disturbance. By combining these criteria, we can also determine approximately when a disturbance began. Areas with declining NDVI over time were identified using simple linear regression in GEE. This tool does not estimate whether a trend is statistically significant (i.e., not due to random chance); thus, it should be considered a qualitative indicator of change and used in conjunction with other measures of change like ΔPN and inspection of the NDVI time series.

To evaluate whether potential areas of concern correspond with areas of poor tree health, we visually examined potential areas of concern in GEE for select sections of the Port Angeles – Sappho (POAN-SAPO; miles 26-36) and Garrison – Taft (GARR-TAFT; miles 38-49) transmission corridors (Figure 5). These corridors were identified by BPA as areas of interest for our analysis because they have experienced recent vegetation fall-in events and are known to have areas of poor tree health. We first visualized areas of concern using a heatmap symbology to facilitate identification of so-called "hot spots", then examined the NDVI time series to determine when the disturbance began and the relative magnitude of the trend. Next, we compared very high-resolution (30-cm to 1-m) aerial imagery from the National Agriculture Imagery Program (NAIP) from before and after to assess whether it coincided spatially with visible tree defoliation, die-off, or otherwise apparent disturbance. NAIP imagery was generally sufficient for our qualitative verification of areas of concern; however, we encountered two

limitations. NAIP imagery is generally collected on a 2-3 year cycle usually during the summer months everywhere in the contiguous US, but unfortunately, much of the area along the POAN-SAPO line was imaged in 2017 and 2023 and the GARR-TAFT line was imaged in 2017, 2021, and 2023; thus, before and after images were sometimes several years from when NDVI time series indicated that change happened. Another limitation of NAIP is that imagery for a given location may be captured during different months from one collection to the next (e.g., August 2017 and October 2023); thus, sometimes it was difficult to determine if the change was associated with disturbance or other non-disturbance phenomena like phenological change or sun angle.

Figure 5. The central map shows the relative location of POAN-SAPO and GARR-TAFT transmission line segments within the BPA service territory. The left map highlights POAN-SAPO line segments (miles 26-36), and the right map highlights GARR-TAFT line segments (miles 38-49), which were identified by BPA as areas with signs of unhealthy vegetation.

3.0 Results & Discussion

Here, we present results on: 1) different ΔPN change metrics; 2) ΔPN threshold determination based on LANDFIRE-mapped "insect/disease" disturbances; and 3) qualitative evaluation of ΔPN and NDVI trend analysis for identifying potential areas of concern.

3.1 Delta Peak NDVI Change Metrics

We reviewed boxplots of three different delta peak NDVI (ΔPN) metrics stratified by disturbance severity and time relative to disturbance to evaluate which would be most useful for detecting poor tree health (Figure 6). Time relative to disturbance was assessed for the year before, year during, and year after disturbance. For all three ΔPN metrics, the magnitude and timing of response were more pronounced with increasing disturbance severity. Areas classified as "low" severity showed little to no difference in ΔPN values before, during, or after disturbance, indicating these metrics may not be sensitive enough to detect subtle disturbance. The more static metrics ($\Delta_{Med}PN$ and $\Delta_{2016}PN$) show similar decreasing trends during and after disturbance, whereas the more dynamic $\Delta_{t-1}PN$ metric shows an initial decline in NDVI in the year during disturbance followed by an increase in NDVI the year after. One possible explanation for the apparent rebound in $\Delta_{t-1}PN$ the year after disturbance could be a lagged response in understory vegetation growth due to increased availability of solar energy following overstory loss; however, additional data are needed to confirm this theory. While the $\Delta_{Med}PN$ and $\Delta_{2016}PN$ metrics exhibit similar patterns in response to disturbance, we selected the $\Delta_{Med}PN$ metric for threshold determination because it is more resilient to interannual variation and easier to interpret in terms of above or below normal.

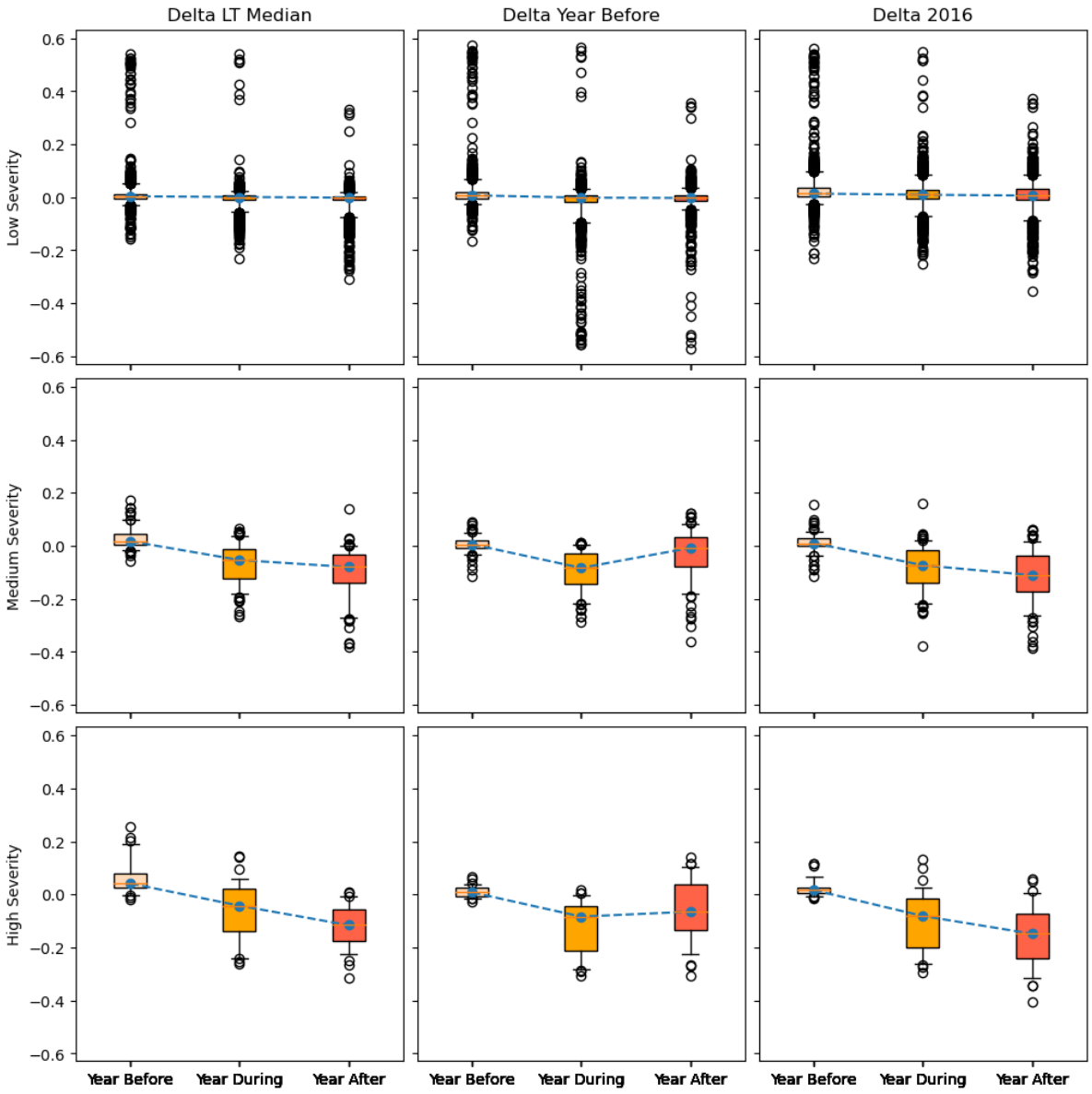

Figure 6. Boxplots of three different ΔPN change metrics for LANDFIRE-mapped insect/disease disturbances. Plots are organized from left to right by metric: delta long-term median ($\Delta_{Med}PN$), delta year before ($\Delta_{t-1}PN$), and delta 2016 ($\Delta_{2016}PN$); and top to bottom by disturbance severity (low, medium, high).

3.2 Delta Peak NDVI Threshold

We reviewed boxplots of $\Delta_{Med}PN$ values for LANDFIRE-mapped insect/disease disturbances and reference locations stratified by disturbance severity and time relative to disturbance (Figure 7) to determine a threshold value for identifying potential areas of concern. All reference locations show little to no difference in $\Delta_{Med}PN$ values across time, indicating they are suitable baseline locations. Except for low severity disturbances, medium and high severity disturbances show obvious declines in $\Delta_{Med}PN$ the year during and year after disturbance compared to reference locations. Given these findings, we chose the median $\Delta_{Med}PN$ "year during" value for

medium-severity disturbances (-0.045) as our threshold for identifying potential areas of concern because it is presumably a more conservative threshold in terms of timing and magnitude.

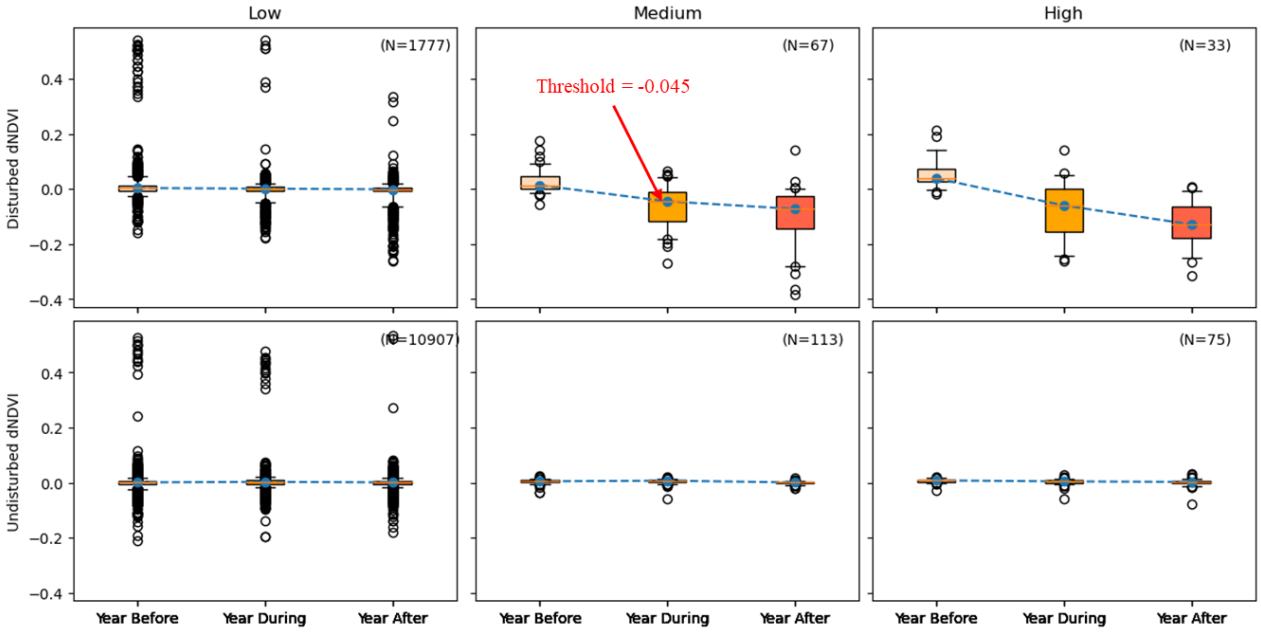

Figure 7. Boxplots of zonal mean $\Delta_{Med}PN$ in the year before, during, and after for LANDFIRE-mapped "insect/disease" disturbances (top row) and undisturbed reference locations (bottom row). Plots are further categorized from left to right by low, medium, and high severity. Blue dashed lines connect the boxplot medians, the whiskers represent the 5th and 95th percentiles, and the dots represent outliers beyond those percentiles.

3.3 Areas of Concern

We mapped potential areas of concern (pixels with negative NDVI trend between 2016-2024 and a $\Delta_{Med}PN$ below -0.045) for two select sections of the POAN-SAPO and GARR-TAFT lines and used before and after NAIP imagery to visually assess whether they coincide with signs of tree defoliation or die-off. We focused primarily on examining so-called "hot spots" where the magnitude of change (as measured by the slope of linear trend analysis and $\Delta_{Med}PN$ value) was more negative and the patch size was greater than ~900 m^2 (3x3 pixels). We acknowledge this biased our review toward areas that are more likely to show signs of defoliation or die-off, but this was appropriate for several reasons. One is that the current ΔPN metrics were more indicative of moderate to high levels of disturbance when compared between LANDFIRE-mapped insect/disease disturbances and reference locations. Second, areas of concern smaller than ~900 m^2 (3x3 pixels) are more likely to be affected by radiometric noise given the spatial resolution (10 m) of Sentinel-2 and not be visible in NAIP imagery. Finally, we assume BPA or other land managers would take a similar approach given the need to quickly identify higher risk areas for closer examination and potential treatment options.

Figures Figure 8 - 11 show examples of locations near (within several kilometers) the POAN-SAPO and GARR-TAFT lines where areas of concern aligned well with visible signs of defoliation or die-off in before/after NAIP images. Inspection of NDVI time series graphs at these locations further confirmed the likelihood of disturbance and provided context about when the disturbance occurred.

Some areas of concern corresponded with other types of disturbance such as landslides, logging, road grading, and flooding (Figure 12 and Figure 13). While it is not surprising that these locations were flagged given the dramatic change in vegetation, it demonstrates how ΔPN metrics are agnostic to disturbance type. Conversely, some potential areas of concern show no visible signs of disturbance and could not be explained. This may be due in part to factors mentioned above regarding the sensitivity of ΔPN metrics and spatial resolution of Sentinel-2 and NAIP imagery, which limits our ability to detect and verify subtle or fine-scale disturbance. However, some areas we suspect are false-positive detections. For example, locations with persistent shadow (e.g., steep north-facing slopes, ecotones between old and new growth forest), which can cause large changes in NDVI, were sometimes flagged as areas of concern (Figure 14). Additionally, some areas of concern overlapped non-forested areas that were not identified as such by our DW tree mask (Figure 15). These areas typically occurred along the edge of forested and non-forested areas, including parts of the transmission corridor. We believe many of these areas can be identified using other data sources and masked in future analyses to reduce false-positives and better constrain the analysis to forested areas.

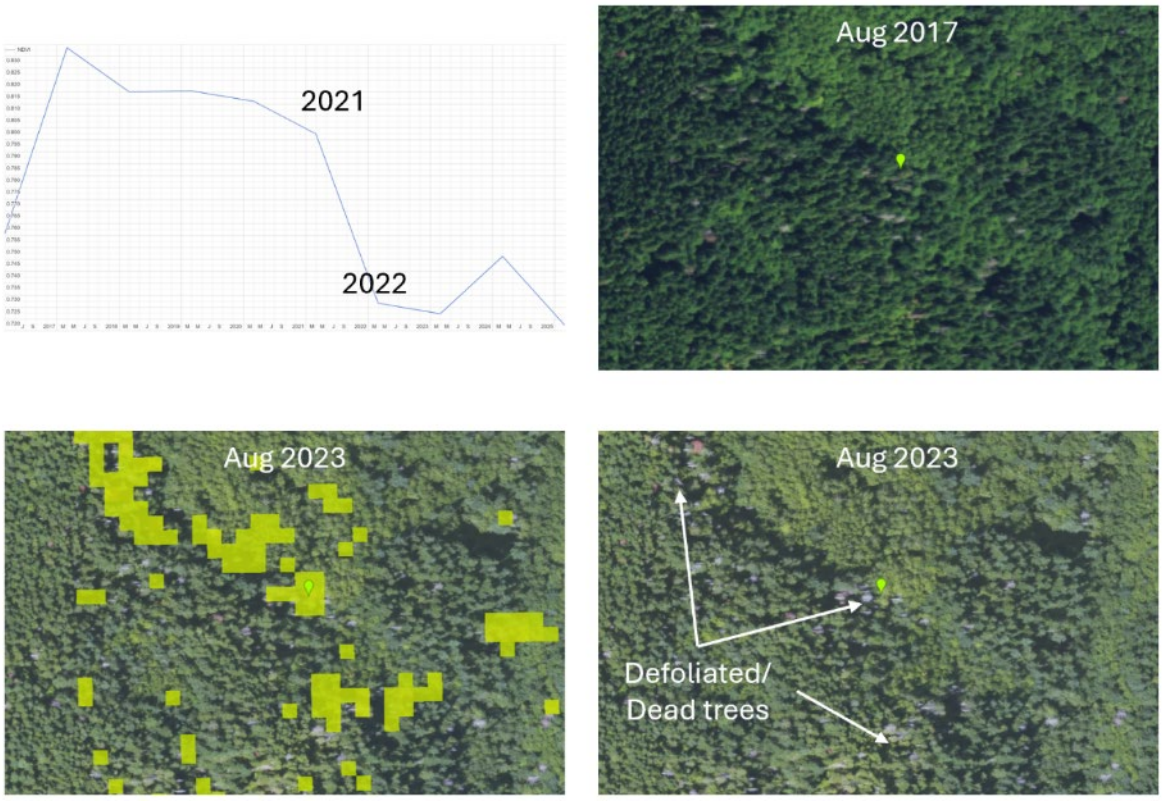

Figure 8. Example area of concern near POAN-SAPO line (124.118168° W, 48.109578° N). NDVI time series corresponds to location of green pin and indicates decline in tree health began between 2021 and 2022. Comparison of NAIP imagery from 2017 (top) and 2023 (bottom) shows expansion of tree defoliation and die-off.

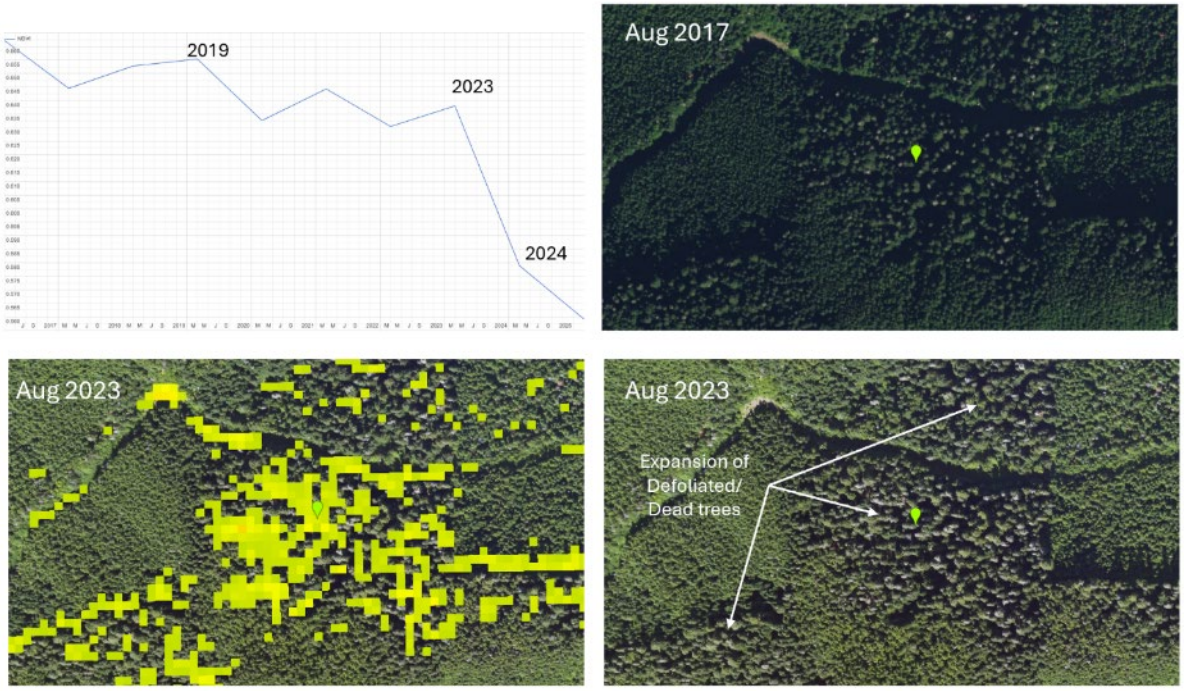

Figure 9. Example area of concern near POAN-SAPO line (124.014879° W, 48.096417° N). NDVI time series corresponds to location of green pin and indicates decline in tree health began as early as 2019 but accelerated between 2023 and 2024. Comparison of NAIP imagery from 2017 (top) and 2023 (bottom) shows increasing severity of tree defoliation and die-off.

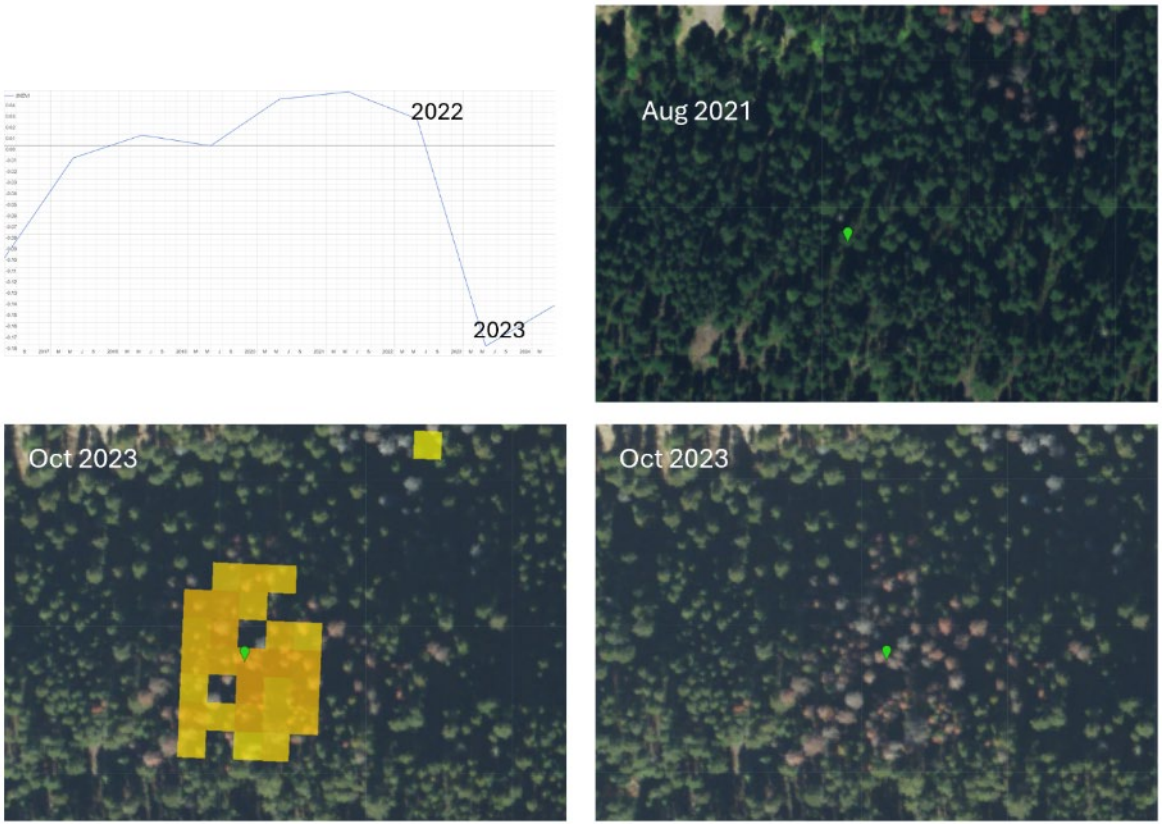

Figure 10. Example area of concern near GARR-TAFT line (113.661686° W, 46.696434° N). NDVI time series corresponds to location of green pin and indicates decline in tree health occurred between 2022 and 2023. Comparison of NAIP imagery from 2021 (top) and 2023 (bottom) shows expansion of tree defoliation and die-off.

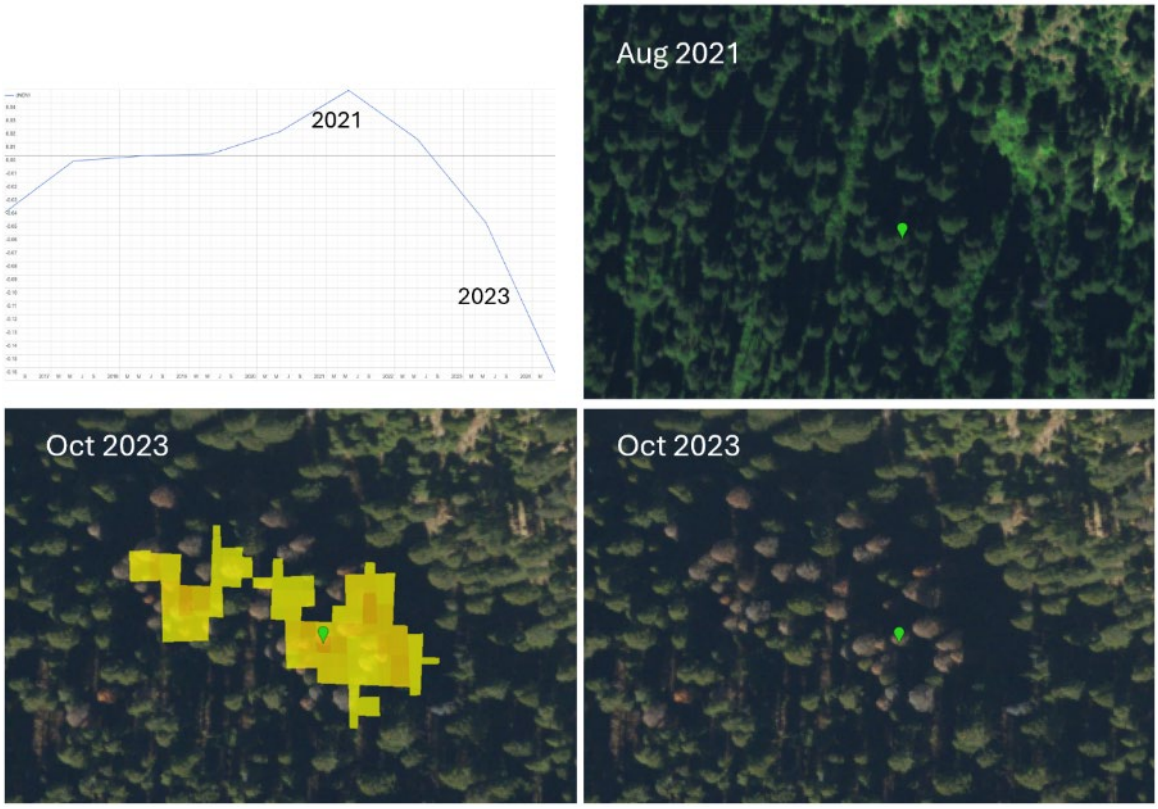

Figure 11. Example area of concern near GARR-TAFT line (113.596140° W, 46.687284° N). NDVI time series corresponds to location of green pin and indicates decline in tree health occurred between 2021 and 2023. Comparison of NAIP imagery from 2021 (top) and 2023 (bottom) shows appearance of tree defoliation and die-off.

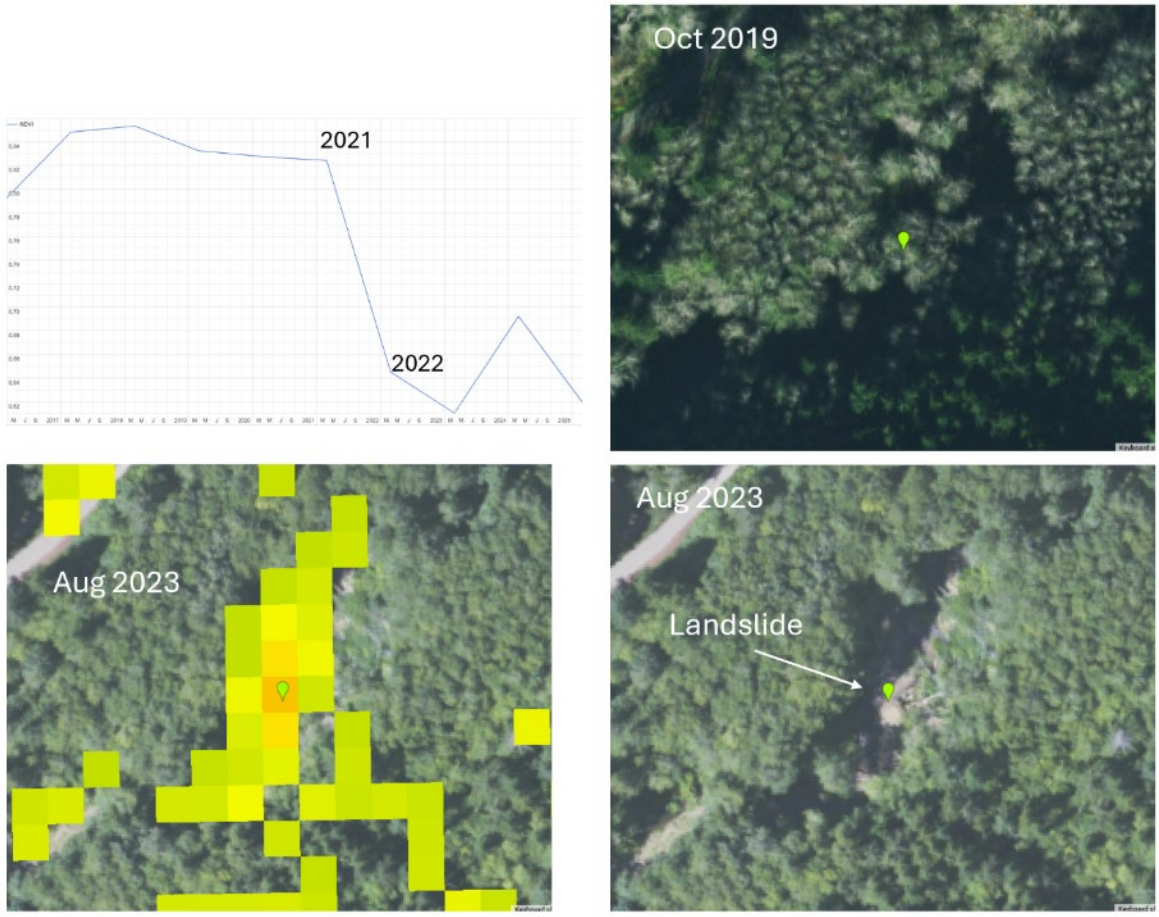

Figure 12. Example area of concern near POAN-SAPO line (124.143765° W, 48.099868° N). NDVI time series corresponds to location of green pin and indicates decline in tree health occurred between 2021 and 2022. Comparison of NAIP imagery from 2019 (top) and 2023 (bottom) shows appearance of a landslide.

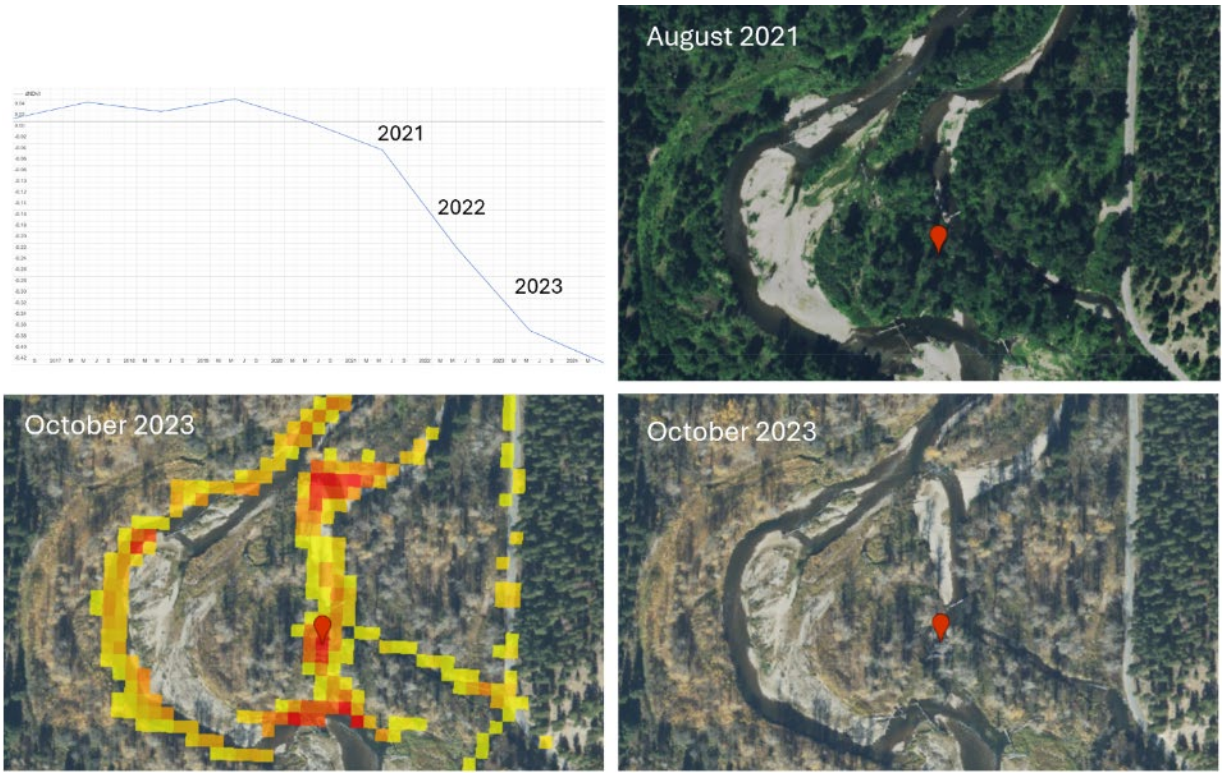

Figure 13. Example area of concern near GARR-TAFT line (113.673946° W, 46.702911° N). NDVI time series corresponds to location of green pin and indicates decline in tree health occurred between 2021 and 2023. Comparison of NAIP imagery from 2021 (top) and 2023 (bottom) shows loss of vegetation and tree die-off due to flood scarring.

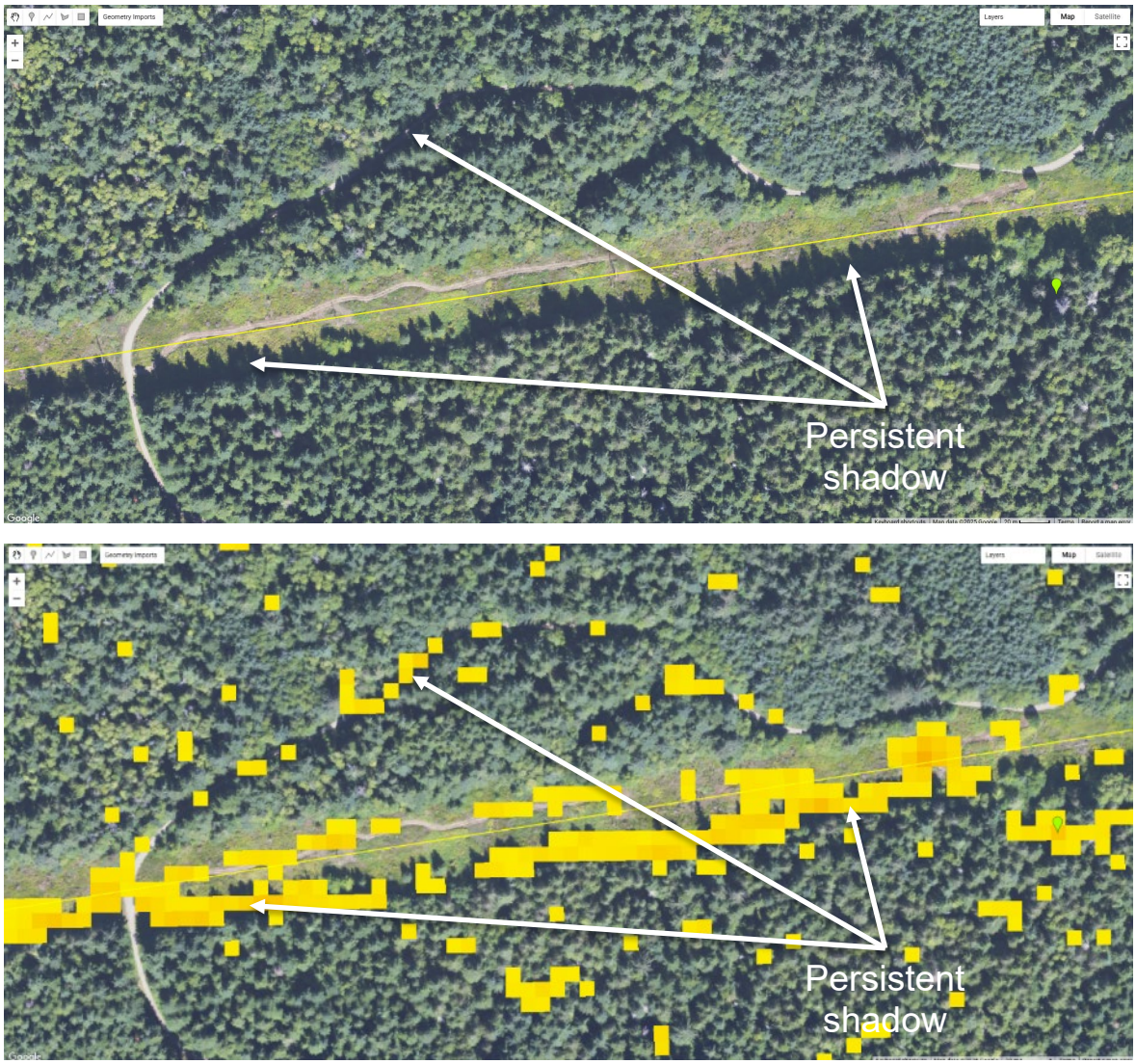

Figure 14. Example area along POAN-SAPO line where persistent shadow is believed to cause false-positive detection.

Figure 15. Example non-forested areas where Dynamic World land cover is misclassified as “tree.” The background image is 2023 NAIP imagery.

4.0 Conclusions

This study presents an initial proof-of-concept for a satellite-based remote sensing approach to identify and monitor potential areas of poor tree health across the entire BPA service territory on an annual basis. Evaluation of vegetation-oriented change detection metrics for known disturbances (as mapped by LANDFIRE) and select sections of the POAN-SAPO and GARR-TAFT transmission lines indicated the method can detect tree defoliation and die-off. However, additional work is recommended to improve model sophistication, noise removal, and validate areas of concern. For example, the sophistication and accuracy of the method could be improved using machine learning techniques and including ancillary data on terrain, plant communities, and interannual climate conditions. Noise can be reduced by improving the non-forest area mask and fine-tuning area of concern criteria. Validation can be improved using other commercial, but Federally accessible sources of high-resolution imagery, LiDAR, and field data. In summary, the approach shows promise for detecting poor tree health adjacent to BPA transmission lines, and because it is scripted in Google Earth Engine, can be applied easily anywhere in the entire service territory.

5.0 References

Brown, C.F., Brumby, S.P., Guzder-Williams, B. et al. Dynamic World, Near real-time global 10 m land use land cover mapping. Sci Data 9, 251 (2022). https://doi.org/10.1038/s41597-022-01307-4

Pacific Northwest National Laboratory

902 Battelle Boulevard
P.O. Box 999
Richland, WA 99354

1-888-375-PNNL (7665)

www.pnnl.gov